High-Sensitive Thermal Sensor Based on a 1D Photonic Crystal Microcavity with Nematic Liquid Crystal

Haouari Charik[1, 2], Mounir Bouras[1, 2, *], and Hamza Bennacer[1, 3]

Abstract—In this study, 1D Photonic Crystal (PhC) with Nematic Liquid Crystal (N-LC) central microcavity is analyzed and discussed using Rigorous Coupled Wave Analysis (RCWA) method. A microcavity is inserted into the 1D PhC by the Air Defect, making it ideal for measuring the properties of an N-LC contained inside the microcavity. Here simulation is considered for NLC (E7) as a thermal sensor. The principle of photonic crystal thermal sensor operation is studied in the TE mode of the incident beam. We conduct a detailed study of the thermal sensor with differences in the width of central microcavity of N-LC. The sensitivity and quality factor are evaluated. Compared to other photonic crystal sensors mentioned previously, this thermal optical sensor has a much simpler structure and higher sensitivity.

1. INTRODUCTION

In recent years, PhCs structures have drawn growing interest [1–4]. The PhCs are periodicities of dielectrics that can control the propagation of electromagnetic wave travelling through them [1]. The periodic variation of their physical properties (dielectric constant) leads to photonic bands of wavelengths at which the light can propagate or be reflected [2, 3]. Diverse structures have been investigated as optical sensors, such as gas sensors [4, 5], mechanical sensors [6], biochemical sensors [7, 8], and refractive index sensors [9–12]. They are used in light flow control systems, such as waveguides, optical fibres, and optical filters [13–15].

Optical sensors can be used in a range of electronic, analytical, and environmental applications. In recent years, their applications as a sensor based on the structure of liquid crystal photonic crystal have experienced a growing development; these rapid developments in photonic technology have greatly improved the efficiency of detection, particularly in the areas of light-liquid interaction and system miniaturization. Any of these optical sensors measure optical property differences as a result of a difference in the refractive index and the material width of a liquid or gas [16].

To obtain one, two, and three-dimensional photonic crystals, different materials and methods have been used [17]. The periodic variation of their physical properties (dielectric constant) leads to photonic bands of wavelengths at which the light can propagate or be stopped [18]. 1D PhCs have gained a lot of interest for the fabrication of various components in silicon-based photonic integrated circuits at IR wavelength due to easy fabrication [23, 26]. The study and design of easily produced PhCs with N-LC central microcavity at optical frequencies have shown increasing interest [27, 28].

PhC doped with N-LC material has recently acquired a great deal of research attention [19–25]. With crystal form orientation, the molecules of the N-LC have a degree of ordering [26]. Because of its optoelectric qualities and temperature sensitivities, the N-LC has a wide range of applications. The 1D

PhC described in these studies has two wide photonic bandgaps from 400 nm to 650 nm and 850 nm to 1900 nm wavelength scales.

Besides, the polarization orientation of the light propagated in 1D PhC N-LC can be regulated by the direction of the applied electric field [21]. Additionally, Lai et al. reported the spectral properties of an electrically tunable 1D PhC infiltrated with twisted N-LC [5]. Dielectric multilayer structures containing N-LCs have been used in a wide range of applications [27–30].

In this paper, a 1-D dielectric multilayer with N-LC defect is investigated for a refractive index thermal sensor of N-LC at an infrared wavelength region. It is necessary for certain photonic devices operating in the infrared region to understand the N-LC refractive indices in this light region. The layers of selected materials are used in the present structure to achieve high contrast between the high refractive index of the layers and to provide a high optical field in the central microcavity [16]. In order to potentially use the given structure as a thermal sensor, the microcavity is modified with different values of defect width W_{Lc}.

The effect of structural parameters on the efficacy of the design proposed has been investigated.

Meanwhile, by optimizing the parameters of the N-LC central defect layer with different thermal sensor widths, greater transmission performance can be realized. We can achieve a higher resolution and broader measurement spectrum of RI with this structure.

2. THEORY AND PRINCIPLE

The structure under study, shown in Fig. 1, a finite-size periodic multilayers structure, consists in the form of (H)(LH)3(N-LC)(HL)3(H), where H = Si, L = Air and an N-LC layer of type (E7) embedded at the central defect. Assuming the anisotropic molecules' optical axis in the X-Z-plane, the N-LC medium dielectric tensor is given by [31]:

$$\varepsilon = \begin{bmatrix} n_e^2\cos^2\emptyset + n_o^2\sin^2\emptyset & 0 & (n_e^2 - n_o^2)\sin\emptyset\cos\emptyset \\ 0 & n_e^2 & 0 \\ (n_e^2 - n_o^2)\sin\emptyset\cos\emptyset & 0 & n_o^2\cos^2\emptyset + n_e^2\sin^2\emptyset \end{bmatrix}$$

In the above equations, the angle between the optical axis of the anisotropic molecules and the z-direction is called tilt angle $\emptyset$ [31].
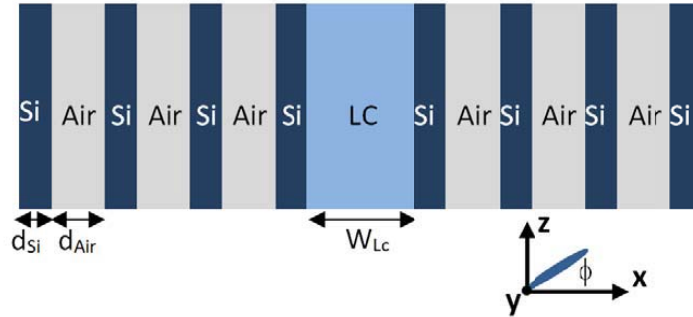
Figure 1. Cross-section of N-LC central defect layer of the 1D PhC structure.

As bias voltage V is applied, under the application of an electric field, liquid crystal molecules rotate $\emptyset$ degrees.

The refractive index for the extraordinary light n_{eff} of each layer is changed with the voltage applied, as well as the light propagating along with the liquid crystal. Their values are given by [32],

$$n_{eff} = \sqrt{\frac{n_e^2 n_o^2}{n_e^2\cos^2\emptyset + n_o^2\sin^2\emptyset}}$$

Thus, modulation of the liquid crystal permittivity is realized. That is, the electrical field produced by the bias voltage changes the permittivity of the liquid crystal [32].

Thermotropic liquid crystals are used for most N-LC based applications. The electro-optic properties of liquid thermotropic crystals are temperature-dependent [33, 34].

The refractive indices, in particular, the extraordinary refractive index n_e, are also temperature sensitive. There is no linear relationship between temperature and n_e, or between temperature and n_o. We will define the resonance wavelength of the thermal sensor of which there is a linear relationship between the resonance wavelength and temperature [35–38].

In the case of E7, the measured ordinary n_o and extraordinary n_e refractive indices show that n_e still decreases as the temperature rises, while n_o first decreases modestly and only increases after the temperature passes 50°. The effective index is n_e when the electric field is added to the N-LC [33]. For this purpose, the peculiar beam would be used in the method of thermal sensing.

At an operating wavelength of 1550 nm, the extraordinary n_e refractive indices decreases from 1,710 to 1,580 by changing the temperature from 15.6°C to 49.6°C [33]. The n_o ordinary refractive indices vary between increase and decrease as the temperature increases from 1.50 to 1.5180 [33, 34]. The influence of the N-LC layer's angle $\emptyset$ on the propagation properties of the proposed design will first be studied.

Due to changes in the rotation angle $\emptyset$ of the N-LC layer, the transition between these modes of operation is $\emptyset = 0°$, $\varepsilon_r = \begin{bmatrix} n_e^2 & n_o^2 & n_o^2 \end{bmatrix}$ while at $\emptyset = 90°$, $\varepsilon_r = \begin{bmatrix} n_o^2 & n_e^2 & n_e^2 \end{bmatrix}$ as shown in Fig. 2.
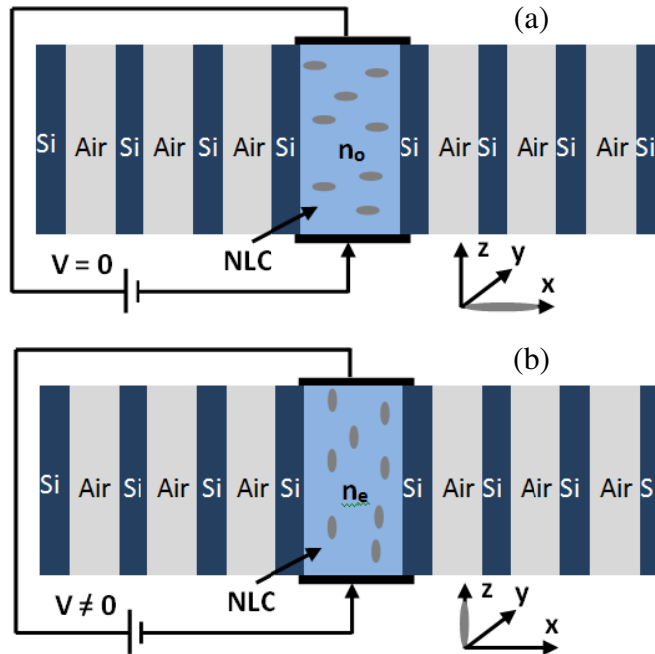

Figure 2. Working principle diagram of the N-CL. At the (a) $\emptyset = 0°$ and (b) $\emptyset = 90°$ of the 1D PhC microcavity structure.

3. RESULTS AND DISCUSSIONS

The influence of the geometrical parameters of the structure on the efficiency of the proposed design has been investigated using 1D PhC N-LC central microcavity content for our transmission calculations and electromagnetic field sensitivity. The influence of the geometrical parameters of the structure on the efficiency of the proposed structure has been tested to analyze 1D PhC N-LC defect content for our transmission measurements and electromagnetic field sensitivity. For an estimate of structure, the RCWA is conducted, and it is enhanced with Modal Transmission Line (MTL) theory.

By compressing the plot horizontally to a single point, we can represent the band structure as a series of vertical lines. We can then vary a design parameter and observe how the distribution of gaps and bands changes.
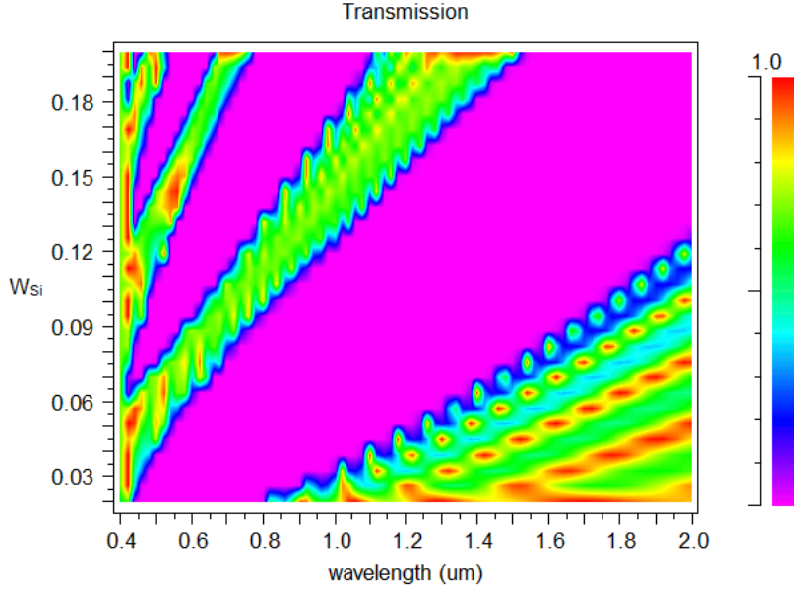
Figure 3. 1D PhC bandgap map.

Fig. 3 shows the resulting gap map where for each value of widths of the dielectric layers (Si), the different colours indicate which polarization of gap, if any, was found. The gap map indicates that the TE gap (Purple) exists over a much wider bandgap. It is also easy to identify the optimum W_{si} for a joint gap. In this simulation, the width of the dielectric layers (Air) is fixed to 200 nm.

Transmission from the microcavity is seen in Fig. 4, with varying cavity widths. By changing the cavity width, the wavelength of the cavity mode in the bandgap (shown in Fig. 3) can be adjusted from 0.85 to 1.85 μm.
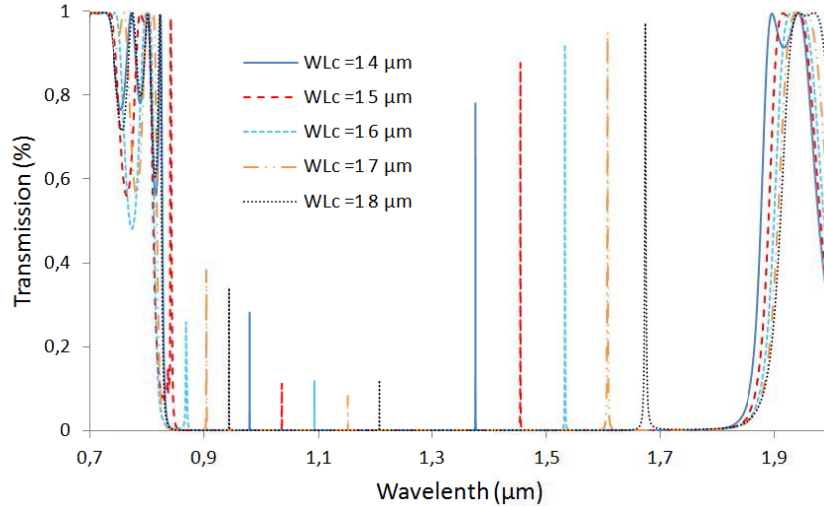

Figure 4. 1-D photonic crystal air cavity transmission with $W_{si} = 0.1 \,\mu\text{m}$ and $W_{\text{Air}} = 0.2 \,\mu\text{m}$. For cavity lengths of 1.4–1.8 μm, different modes oscillate (from left to right).

One will use an external electrical field on the NLC layer to analyze this structure for N-LC Thermo sensing applications, as seen in Fig. 2(b), angle of rotation $\emptyset = 90°$, and $\varepsilon_r = \begin{bmatrix} n_e^2 & n_e^2 & n_e^2 \end{bmatrix}$ is obtained. A laser diode optical signal is then coupled by a lensed fibre into the photonic crystal microcavity. The coupling loss would then be minimized, and the signal emitted would be measurable. A microscope
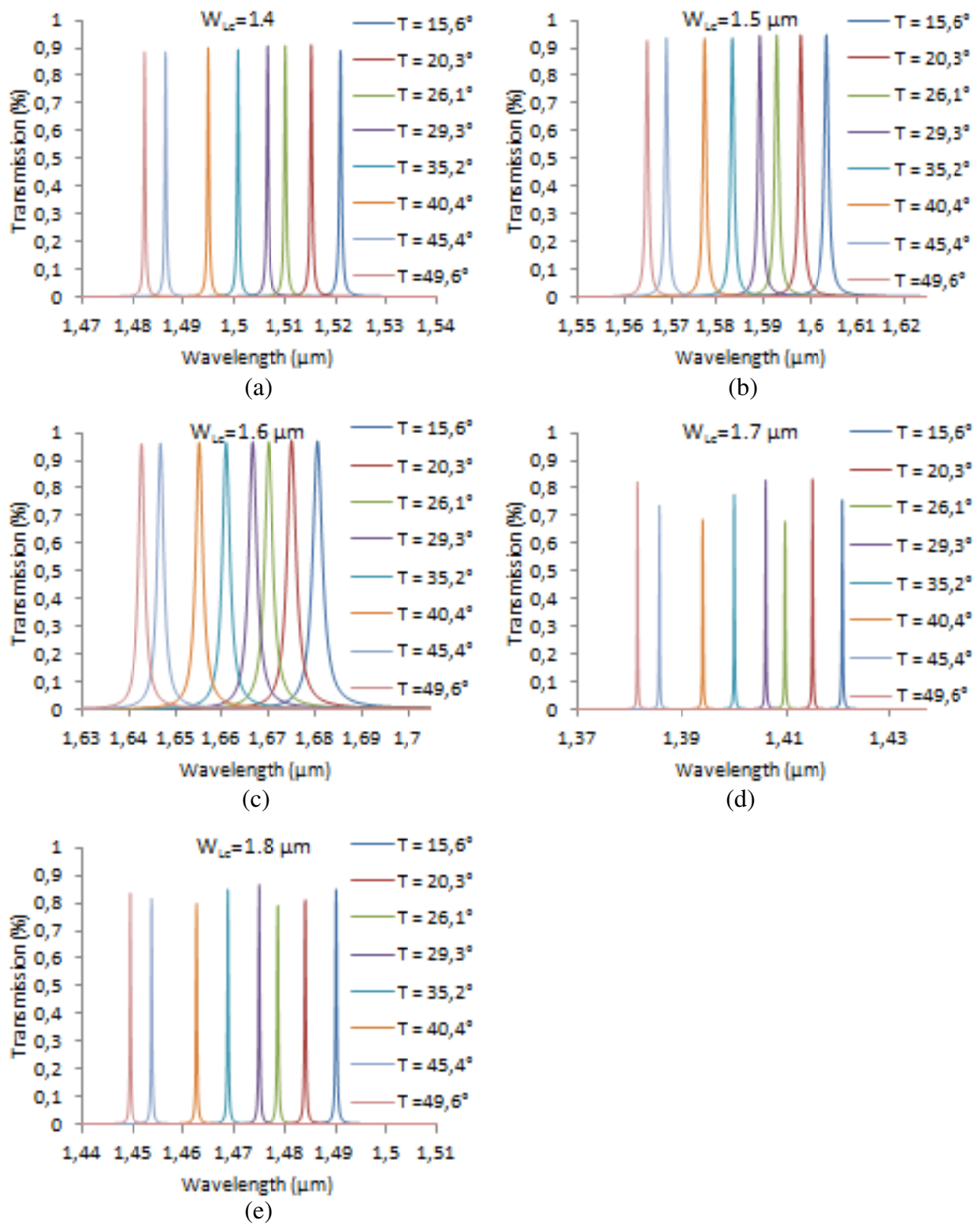
Figure 5. Wavelength-dependent TE mode transmission at differing temperatures and widths (a) $W_{\text{Lc}} = 1.4\,\mu\text{m}$. (b) $W_{\text{Lc}} = 1.5\,\mu\text{m}$. (c) $W_{\text{Lc}} = 1.6\,\mu\text{m}$. (d) $W_{\text{Lc}} = 1.7\,\mu\text{m}$. (e) $W_{\text{Lc}} = 1.8\,\mu\text{m}$.
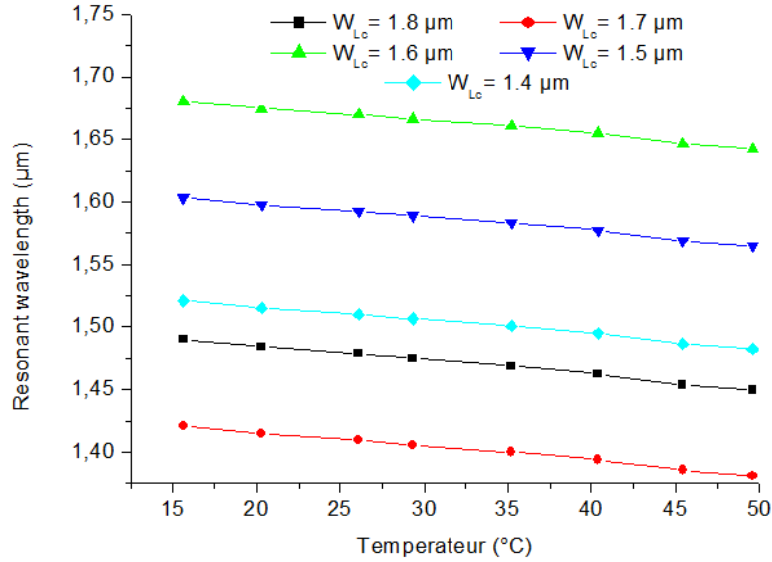
Figure 6. Resonant wavelength shift as a function of temperature (TE mode).

target absorbs the light emitted from the defect, which is then detected using a photodiode [16].

The thermal sensors are supposed to be in contact with the external electric field. The authorized transmission modes in 1D N-LC PhC are shown in Figs. 5 and 6 at different N-LC widths. The TE allowed mode is at N-LC widths of 1.4, 1.5, 1.6, 1.7, and 1.8 µm.

The microcavity, which is shifted into the bandgap as the N-LC widths are modified, enables a single defect mode. When a different temperature is considered in the defect mode, wavelength shifts occur. This results in a shift in the range of output propagation that corresponds to the RI change.

Figure 6 indicates that the resonance wavelength is greatly influenced by the variation in the width and temperature of the design N-LC defect layer. The sensitivity of the proposed thermal sensor would also be influenced by the width and temperature.

Sensitivity and quality factor are essential criteria for determining the efficiency of a thermal sensor. The sensitivity S of the thermal sensor is defined by $\Delta\lambda/\Delta T$, where $\Delta\lambda$ is the wavelength shift of defect mode, and ΔT is the temperature change and measured in nm/°C unit.

Figure 7 shows the calculated temperature sensitivity and quality factor of the proposed thermal sensor with different N-LC defect layer widths for TE mode.

Furthermore, the effect of the change of the defect's width on the sensitivity of the proposed 1-D PhC is very weak as shown in Fig. 7. A monotonic wavelength response has been declared in the sensitivity analysis and enhanced by increasing the Width microcavity. Thence to increase the sensitivity of the present structure, the sensitivity values for the width of microcavity $W_{\mathrm{Lc}} = 1.6\,\mu\mathrm{m}$ ($S_3 = 1.38\,\mathrm{nm/°C}$) are higher than the width of microcavity for (1.4, 1.5, 1.7, 1.8 µm) ($S_1 = 1.23\,\mathrm{nm/°C}$, $S_2 = 1.27\,\mathrm{nm/°C}$, $S_4 = 1.33\,\mathrm{nm/°C}$, $S_5 = 1.3\,\mathrm{nm/°C}$), respectively.

The quality factor is seen in Fig. 7 (black line), as a function of the length of the cavity. The quality factor decreases by increasing the defect width. The offered QF at $W_{\mathrm{Lc}} = 1.4\,\mu\mathrm{m}$ is equal to 5012. For sensing applications, a narrow bandwidth mode is desirable, and we must also select the parameters in such a way that the quality factor peaks at the operation's wavelength.

From Fig. 6, if we assume that the relationship between the resonance shift and the RI is roughly linear, the resonance shift is defined by the following equation for a given liquid index to predict resonance frequency after linear fitting of simulation data for ($W_{\mathrm{Lc}} = 1.6\,\mu\mathrm{m}$):

$$y_3\,[\mu\mathrm{m}] = (-0.0013T + 1.6984)\,[\mu\mathrm{m}]$$

We determined the resonance wavelength of the thermal sensor and found a linear relationship between the temperature and resonance wavelength. The linearity of the resonance wavelength curve is about $R^2 = 0.9932$, indicating high linearity of the thermal sensor.
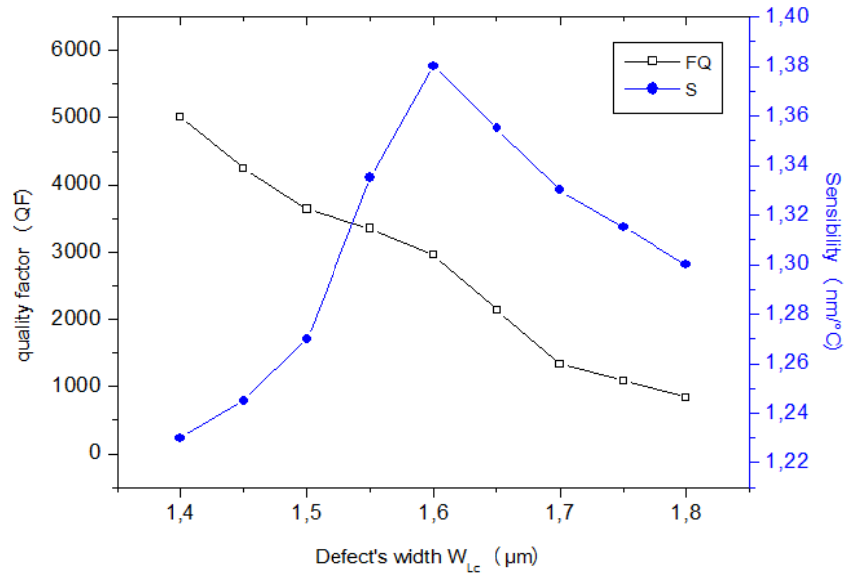
Figure 7. The quality factor and sensitivity as a function of liquid crystal width for TE mode.

In comparison with other thermal sensors using PhCs, our proposed thermal sensor has higher sensitivity (Table 1).

Table 1. Comparison of the proposed structure with different designs of PhCs sensor.

References	Type of device	Sensibility (nm/°C)
[1]	PhC-1D cavity for central defect layer with a SiO_2	0.0037
[1]	PhC-1D cavity for one defect layer with a $Bi_4Ge_3O_{12}$	0.0050
[3]	PhC-1D cavity with a dielectric-superconducting pair defect	0.012
[16]	PhC-1D central N-LC defect with MLC-9200 materiel for TE mode	0.328
[16]	PhC-1D central N-LC defect with a MLC-9200 materiel for TM mode	0.316
[29]	PhC-1D cavity for two defects layers with a $Bi_4Ge_3O_{12}$	0.00004
This work	PhC-1D central N-LC defect with an (E7) materiel for TE	1.38

4. CONCLUSION

For RI sensing of N-LC at an infrared wavelength field, a 1D dielectric multilayer microcavity is studied. To create a cavity, an air-central defect is used. The detection theory is based on the resonance shift of the resonance of the N-LC central defect layer as a function of the RI, which leads to a shift in the output transmission spectrum. The effect of the adjustment in structural parameters on the proposed structure has been investigated to provide better sensitivity and quality factor.

To enhance the sensitivity and resolution of the thermal sensor, a method is presented. A thermal sensor can be obtained in the desired wavelength range by choosing the acceptable value of the geometric parameters of the structure proposed.

We find that this design has a higher sensitivity and quality factor than the other structures, and the resonance wavelength changes by 0.1386 nm for $n = 0.1°C$. The sensor sensitivity can reach 1.38 nm/°C, and the transmission efficiency can reach 95–97% in the 15–50°C temperature range. The thermal sensor attributed to the largest N-LC defect used here has a simple structure with such a width of 1.6 µm and can be integrated into photonic circuits based on silicon.

ACKNOWLEDGMENT

REFERENCES

1. Chang, Y. H., Y. Y. Jhu, and C. J. Wu, "Temperature dependence of defect mode in a defective photonic crystal," *Optics Communications*, Vol. 285, No. 6, 1501–1504, 2012.
2. Bougriou, F., et al., "Optofluidic sensor using two-dimensional photonic crystal waveguides," *Eur. Phys. J. Appl. Phys.*, Vol. 62, No. 1, 11201–11205, 2013.
3. Wu, J. J. and J. X. Gao, "Low temperature sensor based on one-dimensional photonic crystals with a dielectric-superconducting pair defect," *Optik*, Vol. 126, No. 24, 5368–5371, 2015.
4. Ma, L., T. Katagiri, and Y. Matsuura, "Surface-plasmon resonance sensor using silica-core Bragg fiber," *Opt. Lett.*, Vol. 34, No. 7, 1069–1071, 2009.
5. Lai, W., S. Chakravarty, X. Wang, C. Lin, and R. T. Chen, "On-chip methane sensing by near-IR absorption signatures in a photonic crystal slot waveguide," *Opt. Lett.*, Vol. 36, 984–986, 2011.
6. Zhang, Y., Y. Zhao, and Q. Wang, "Measurement of methane concentration with cryptophane E infiltrated photonic crystal microcavity," *Sens. Actuators B: Chem.*, Vol. 209, 431–437, 2015.
7. Chang, Y., Y. Jhu, and C. Wu, "Temperature dependence of defect mode in a defective photonic crystal," *Optics Communications*, Vol. 285, 1501–1504, 2012.
8. Zhang, Y., Y. Zhao, and R. Lv, "A review for optical sensors based on photonic crystal cavities," *Sens. Actuators A: Phys.*, Vol. 233, 374–389, 2015.
9. Liu, Y. and H. W. M. Salemink, "All-optical on-chip sensor for high refractive index sensing in photonic crystals," *EPL*, Vol. 107, Nos. 1–5, 34008, 2014.
10. Zheng, S., B. Shan, M. Ghandehari, and J. Ou, "Sensitivity characterization of cladding modes in long-period gratings photonic crystalfiber for structural health monitoring," *Measurement*, Vol. 72, 43–51, 2015.
11. Zheng, S., Y. Zhu, and S. Krishnaswamy, "Nanofilm-coated photonic crystal fiber long-period gratings with modal transition for high chemical sensitivity and selectivity," *SPIE*, Vol. 8346, 83460D, 2012.
12. Fenzl, C., T. Hirsch, and O. S. Wolfbeis, "Photonic crystals for chemical sensing and biosensing," *Angew. Chem. Int. Edit.*, Vol. 53, 3318–3335, 2014.
13. Gong, Q. H. and X.-Y. Hu, "Ultrafast photonic crystal optical switching," *Front. Phys. China*, Vol. 1, 171, 2006.
14. Singh, A., K. B. Thapa, and N. Kumar, "Analysis and design of optical biosensors using one-dimensional photonic crystals," *Optik*, Vol. 126, No. 2, 244–250, 2015.
15. Awasthi, S. K. and S. P. Ojha, "Design of a tunable optical filter by using a one-dimensional ternary photonic band gap material," *Progress In Electromagnetics Research M*, Vol. 4, 117–132, 2008.
16. Mohebbi, M., "Refractive index sensing of gases based on a one-dimensional photonic crystal nanocavity," *J. Sens. Sens. Syst.*, Vol. 4, No. 1, 209–215, 2015.
17. Sakoda, K., *Optical Properties of Photonic Crystals*, Vol. 80, Springer Science & Business Media, 2004.
18. Skorobogatiy, M. and J. Yang, *Fundamentals of Photonic Crystal Guiding*, Cambridge University Press, 2009.
19. Mounir, B., C. Haouari, A. Saïd, and A. Hocini, "Analysis of highly sensitive biosensor for glucose based on a one-dimensional photonic crystal nanocavity," *Optical Engineering*, Vol. 58, No. 2, 027102, 2019.
20. Wu, P. C. and W. Lee, "One-dimensional photonic crystals containing memory-enabling liquid crystal defect layers," *Proc. SPIE*, Vol. 8828, 1–10, 2013.

21. Mohamed, M. S., M. F. O. Hameed, M. M. El-Okr, and S. S. A. Obayya, "Characterization of one-dimensional liquid crystal photonic crystal structure," *Optik*, Vol. 127, 8774–8781, 2016.

22. Bouras, M. and A. Hocini, "Mode conversion in magneto-optic rib waveguide made by silica matrix doped with magnetic nanoparticles," *Optics Communications*, Vol. 363, 138–144, 2016.

23. Marthandappa, M. and R. Somashekar, Nagappa, "Electro-optic effects in nematic liquid crystals," *Phy. State Sol. (A)*, 127–259, 1991.

24. Armand, H. and M. D. Ardakani, "Theoretical study of liquid crystal dielectric-loaded plasmonic waveguide," *International Journal of Microwave and Wireless Technologies*, Vol. 9, No. 2, 275, 2017.

25. Liu, Y., Y. Liu, H. Li, D. Jiang, W. Cao, H. Chen, L. Xia, and R. Xu, "Tunable microwave bandpass filter integrated power divider based on the high anisotropy electro-optic nematic liquid crystal," *Review of Scientific Instruments*, Vol. 87, 074709, 2016.

26. Li, J., C. H. Wen, S. Gauza, R. Lu, and S. Wu, "Refractive indices of liquid crystals for display applications," *IEEE/OSA J. Disp. Technol.*, Vol. 1, 51–61, 2005.

27. Li, J., S.-T. Wu, B. Stefano, M. Riccardo, and F. Sandro, "Infrared refractive indices of liquid crystals," *J. Appl. Phys.*, Vol. 97, 073501, 2005.

28. Li, J. and S. T. Wu, "Extended Cauchy equations for the refractive indices of liquid crystals," *Appl. Phys.*, Vol. 95, 896, 2004.

29. Bouzidi, A. and D. Bria, "Low temperature sensor based on one-dimensional photonic crystals," *International Conference on Electronic Engineering and Renewable Energy*, 157–163, Springer, Singapore, 2018.

30. Hocini, A., M. Bouras, and H. Amata, "Theoretical investigations on optical properties of magneto-optical thinfilm on ion-exchanged glass waveguide," *Opt. Mater.*, Vol. 35, No. 9, 1669–1674, 2013.

31. Dermeche, N., M. Bouras, and R. Abdi-Ghaleh, "Existence of high Faraday rotation and transmittance in magneto photonic crystals made by silica matrix doped with magnetic nanoparticles," *Optik*, Vol. 198, 163225, 2019.

32. Liu, Y., Y. Liu, H. Li, D. Jiang, W. Cao, H. Chen, L. Xia, and R. Xu, "Tunable microwave bandpass filter integrated power divider based on the high anisotropy electro-optic nematic liquid crystal," *Review of Scientific Instruments*, Vol. 87, 074709, 2016.

33. Mounir, B., C. Haouari, A. Saïd, and A. Hocini, "Analysis of highly sensitive biosensor for glucose based on a one-dimensional photonic crystal nanocavity," *Optical Engineering*, Vol. 58, No. 2, 027102, 2019.

34. Li, J. and S. T. Wu, "Extended Cauchy equations for the refractive indices of liquid crystals," *Appl. Phys.*, Vol. 95, 896, 2004.

35. Monmayrant, A., et al., "Full optical confinement in 1D mesoscopic photonic crystal-based microcavities: An experimental demonstration," *Optics Express*, Vol. 25, No. 23, 28288–28294, 2017.

36. D'orazio, A., "Infiltrated liquid crystal photonic bandgap devices for switching and tunable filtering," *Fiber and Integrated Optics*, Vol. 22, No. 3, 161–172, 2003.

37. Perova, T. S., et al., "Tunable one-dimensional photonic crystal structures based on grooved Si infiltrated with liquid crystal E7," *Phy. State Sol. (C)*, Vol. 4, No. 6, 1961–1965, 2007.

38. Miroshnichenko, A. E., E. Brasselet, and Y. S. Kivshar, "All-optical switching and multistability in photonic structures with liquid crystal defects," *Applied Physics Letters*, Vol. 92, No. 25, 230, 2008.